Vol.69: e26260150, 2026
https://doi.org/10.1590/1678-4324-2026260150
ISSN 1678-4324 Online Edition

BABT
Brazilian Archives of Biology and Technology

*Article - Agricultural Technologies, Biotechnology and Environment*

# Production and Characterization of Biodegradable Films Based on Starch and Cellulose Nanofibrils from Pearl Millet (*Cenchrus americanus* (L.) Morrone)

**Luana Carolina Ruths**[1]
https://orcid.org/0009-0001-3972-1097

**Ivan Venson**[2]
https://orcid.org/0000-0002-4368-8779

**Lemuel Cordeiro**[1]
https://orcid.org/0009-0001-7322-9995

**Luís Antônio Pinheiro**[3]
https://orcid.org/0000-0001-5068-3725

**Stephanie Schiavo Romko**[1]
https://orcid.org/0000-0002-0140-7772

**Ivo Mottin Demiate**[1]
https://orcid.org/0000-0002-5609-0186

**Juliana Bonametti Olivato**[1]
https://orcid.org/0000-0001-6463-6380

**Luiz Gustavo Lacerda**[1]*
https://orcid.org/0000-0002-4689-5431

[1]Universidade Estadual de Ponta Grossa, Programa de Pós-Graduação em Ciência e Tecnologia de Alimentos, Ponta Grossa, Paraná, Brasil; [2]Universidade Federal do Paraná, Departamento de Engenharia e Tecnologia Florestal, Curitiba, Paraná, Brasil; [3]Universidade Estadual de Ponta Grossa, Departamento de Engenharia de Materiais, Ponta Grossa, Paraná, Brasil.

Editor-in-Chief: Paulo Vitor Farago
Associate Editor: Bill Jorge Costa

Received: 20-Mar-2026; Accepted: 01-Apr-2026

*Correspondence: lglacerda@uepg.br; Tel.: +55-41-84320018 (L.G.L.).

**HIGHLIGHTS**

- Valorization of pearl millet stalk and seeds for green packaging solutions.
- CNF incorporation improved thermal stability and modified film microstructure.
- CNF:water, (w/w) of 1:500 formulation showed the best balance of mechanical and barrier properties.

**Abstract:** Food packaging, predominantly made from fossil fuel-based plastics, generates significant environmental impacts due to its non-biodegradable nature. An alternative lies in biodegradable films from renewable sources like starch and cellulose. This study aimed to develop and characterize biodegradable films based on starch reinforced with cellulose nanofibrils (CNF), both derived from underutilized pearl millet (*Cenchrus americanus* (L.) Morrone), following a biorefinery and circular economy concept. Films were produced by casting with different dilutions (CNF:water, w/w) of: 1:100, 1:200, 1:500, 1:1000 and 1:2000, along with the control formulation without CNF addition, named F100, F200, F500, F1000, F2000 and F0, respectively. They were characterized for their thermal, morphological, physical and mechanical properties. Results showed that CNF incorporation increased the thermal stability of the films in the first thermal event (from 63.5 °C for F0 up to 81.7 °C for F100). Water vapor permeability decreased, although the difference was not statistically significant, ranging from $8.87\times10^{-11}$ to $1.11\times10^{-10}$ g. $Pa^{-1}$. $s^{-1}$. $m^{-1}$, while the solubility content ranged from 17.4% to 19.5% ($p > 0.05$). The F500 formulation exhibited the best overall mechanical performance, with the highest tensile strength (2.47 MPa), intermediate stiffness (84.1 MPa), and preserved flexibility (118.1%). Conversely, excess CNF in formulation F100 led to agglomerates and compromised mechanical properties. In conclusion, starch and CNF from pearl millet are viable for producing biodegradable films. The F500 formulation, in particular, shows promising potential for application in low and intermediate moisture food packaging, offering a sustainable alternative to conventional plastics.

**Keywords:** food packaging; bioplastic; nanocomposite.

## INTRODUCTION

Food packaging plays a crucial role in protecting products during transport and storage, extending shelf life by acting as a barrier against contamination [1]. Plastics are the most widely used materials for this purpose due to their easy processability and low cost. However, besides being derived from non-renewable sources, these polymers do not degrade in nature, causing significant environmental impacts [2,3].

In response, research has increasingly focused on renewable biopolymers to develop biodegradable films. At the end of their life cycle, these materials degrade naturally without leaving polluting residues, positioning themselves as ecological alternatives capable of meeting the demand for packaging with properties similar to those of conventional plastics [2,3].

Starch-based biodegradable films have emerged as a sustainable option, combining economic viability with raw material availability [4]. However, starch films alone may not always satisfy the required mechanical properties. This limitation necessitates the use of reinforcing materials, such as cellulose, which is more rigid and stable. Cellulose nanofibrils (CNF), obtained through chemical and mechanical treatments of cellulose fibers, are particularly noteworthy. Their nanometric dimensions, when incorporated into films, can significantly enhance mechanical and barrier performance.

Consequently, diverse natural sources of these biopolymers are being investigated. Recent studies have specifically explored the potential of millet as a source of both cellulose and starch-rich grains [5]. Pearl millet (*Cenchrus americanus* (L.) Morrone) [syn. *Pennisetum glaucum* (L.) R.Br] is a plant belonging to the grass family originating in Africa, where it has been cultivated for at least 10,000 years. Despite its long history as a dietary staple for populations in arid and developing regions, providing income for vulnerable families, the plant remains technologically underutilized and underexplored [1,6].

This cereal has become increasingly attractive because of its remarkable adaptability to adverse conditions, such as poor soils, hot climates, and water scarcity, where other crops often fail [5,7]. Given current climate challenges and the growing pressure on natural resources, this resilience positions pearl millet as a promising and economically viable agricultural alternative [1,6].

From a technological perspective, the starch present in millet grains stands out as a renewable source for industrial applications, particularly due to its high amylose content [5]. High amylose content is known to form denser and more cohesive polymeric networks, which can confer greater mechanical strength to materials [8]. These properties can be further optimized by the reinforcing effect provided by cellulose nanofibrils obtained from other millet plant components, such as the stem. This integrated approach broadens the potential for developing high-performance biodegradable packaging materials [9].

Therefore, this study aimed to produce and characterize biodegradable films based on starch reinforced with cellulose nanofibrils, both derived from pearl millet, evaluating their thermal, morphological, physical, and mechanical properties for potential food packaging applications.

## MATERIAL AND METHODS

Pearl millet stalks for cellulose extraction were kindly provided by a farmer from the municipality of Carambeí (24°57'00" S 50°07'16" W), Paraná, Brazil. Starch was extracted from millet seeds of the BRS 1501 cultivar, which were acquired through e-commerce. The plasticizer used was glycerol P.A. (analytical grade). All reagents used in the experiments were of analytical grade.

### Extraction and Characterization of Pearl Millet Starch

Pearl millet starch was isolated by alkaline maceration [10,11]. Pearl millet seeds were washed and homogenized with 0.016 mol/L sodium bisulfite ($NaHSO_3$) solution and deionized water in a 1:1 (w/v) ratio using a blender (MONDIAL, model L-99-FB). Subsequently, the suspension was passed through 150 mesh (0.106 mm) and 270 mesh (0.053 mm) sieves.

The residual liquid from sieving was subjected to immersion in NaOH (1.0 M) at 0.1% (w/v) for 12 h at 4 °C. The precipitated starch was centrifuged (HIMAC, model CR-21 GII) using an R14A rotor at 10,000 × g for 5 min at 4 °C, and the dark upper layer formed was carefully removed by scraping with a spatula. Neutralization was carried out with 1.0 M HCl and the sample was centrifuged under the same conditions. The moist starch was dried in a forced air oven at 40 °C for 24 h, followed by sieving through 150 mesh.

The proximate composition of the starch was determined according to the methodology of the Instituto Adolfo Lutz [12], where moisture content, ash content, protein content (Kjeldahl method), and lipid content (Soxhlet method) were analyzed. The carbohydrate content was calculated by difference to 100%.

Amylose content was determined based on iodine affinity (IA) using a potentiometric autotitrator [13]. Previously defatted samples (100 mg) were mixed with 1 mL of deionized water and 5 mL of KOH (1 N), and the mixture was stirred for 30 min at 25 °C. Methyl orange was used as pH indicator, and HCl (0.5 N) was added as neutralizing solution. Subsequently, 10 mL of KI (0.5 N) and deionized water were added to reach a mass of 100.9 g. Titration was performed using an automatic titrator (Titrino Plus, Metrohm, Switzerland). Amylose content was calculated by dividing the iodine affinity of the starch sample ($IA_s$) by the iodine affinity of pure amylose, considered as 0.2, and multiplying the result by 100%.

**Isolation of Cellulose Nanofibrils from Pearl Millet**

Pearl millet stalks were cut into small chips of approximately 6 cm and dried in an oven at 40 °C. Alkaline pretreatment was employed to obtain a bleached cellulosic pulp [14].

Initially, the pulp was subjected to a sequential treatment with sodium chlorite ($NaClO_2$) in acetate buffer (pH 4.8), carried out in two stages: the first with $NaClO_2$ solution at 23.44 g/L for 2 h at 72 °C, and the second with $NaClO_2$ solution at 100 g/L for 1 h 15 min at 82.5 °C. Between these stages, intercalated treatments with 5% NaOH at 82.5 °C for 1 h were performed, aiming at delignification and fiber purification. This cycle of treatments with $NaClO_2$ and NaOH was repeated three times, including the partial reuse of $NaClO_2$ solutions.

Subsequently, bleaching was carried out with 5% (w/v) NaOH solution and 10% (v/v) hydrogen peroxide ($H_2O_2$) at 80 °C for approximately 1 h. The obtained solution was neutralized with 3% (v/v) acetic acid, filtered, and washed.

The bleached cellulosic pulp was suspended in water and subjected to grinding in a colloidal stone mill (Super Masscolloider - MKCA6-2J) at 1500 rpm. Between 10 and 15 passes were performed until a gel-like suspension was obtained, with a final concentration of 1,5% [15].

The zeta potential of the suspension was determined using a particle analyzer (Malvern / Zetasizer Nano -ZS90). The sample was dispersed in deionized water at different dilutions and subjected to a sonicator bath for 10 min for homogenization and dispersion of the nanofibrils. Measurements were performed at 25 °C at neutral pH [16].

**Preparation and Characterization of Biodegradable Films**

The films were produced using the casting technique [17]. A film-forming solution was prepared by dissolving starch in deionized water, using glycerol as plasticizer and adding cellulose nanofibril suspension as reinforcement.

For film preparation, 1.4 g of starch, 0.35 g of glycerol, and different concentrations of cellulose nanofibril suspension were dispersed in water and mixed. The cellulose nanofibril suspensions were used at dilutions (CNF:water, w/w) of 1:100, 1:200, 1:500, 1:1000, and 1:2000, corresponding to the formulations designated as F100, F200, F500, F1000, and F2000, respectively. For the control film formulation, F0, prepared without the addition of cellulose nanofibrils, the corresponding volume of water was added to complete the total mass of the mixture to 28 g (100%). The mixture was heated to 95 °C to ensure starch gelatinization and maintained under constant stirring (160 rpm) for 5 min using a Rapid Visco Analyzer, RVA-4 (Newport Scientific, Australia). The film-forming solution was poured into polystyrene plates (90 × 15 mm) and dried in an oven with air circulation at 40 °C for 5 h. Subsequently, the plates containing the films were stored in a desiccator with controlled humidity (RH = 53%), using a saturated magnesium nitrate solution [18].

*Thermogravimetric Analysis (TGA)*

Thermogravimetric curves of the films were obtained using TGA-50 thermal analysis system (Shimadzu, Japan). Approximately 6.0 mg of each sample were weighed in open alumina crucibles and heated from 30 to 600 °C under a compressed air flow of 100 mL $min^{-1}$, at a heating rate of 10 °C $min^{-1}$. The equipment was calibrated with a standard weight and calcium monohydrate oxalate. Mass variations as a function of temperature were determined using the TA-60 WS data analysis software, which was also used to determine derivative thermogravimetry (DTG) [19].

*Scanning Electron Microscopy (SEM)*

To evaluate the microstructure of the biodegradable films, a Vega 3 scanning electron microscope (Tescan, Czech Republic) was used. Samples of 1 $cm^2$ were stored in a desiccator (0% RH) containing calcium chloride for seven days prior to analysis. The film samples were fixed onto carbon tape and sputter-coated with gold and palladium (150 s; 20 mA) to promote an electron-conductive surface [20].

*Water Vapor Permeability and Water Solubity*

The water vapor permeability of the films was determined by the gravimetric method, according to ASTM E-96-95 [21]. Circular samples (3 cm in diameter) had their thickness measured with a digital micrometer (Mitutoyo, Japan; precision 0.001 mm). Each sample was fixed onto jars containing 3.75 g of anhydrous calcium chloride (0% RH). The jars were kept in a desiccator with saturated sodium chloride solution (75% RH) at 25 °C. Successive weighings were performed over four days [17]. WVP values were expressed in g. $s^{-1}$. $m^{-1}$. $Pa^{-1}$, calculated from the mass gain through the permeation area, considering time, thickness, and the water vapor partial pressure difference (1753.55 Pa).

The water solubility of the films was evaluated by the gravimetric method [22]. Samples of 4 cm² were previously dried (105 °C/24 h) to obtain the initial dry mass and immersed in 50 mL of deionized water at 25 °C for 24 h. After this period, the insoluble material was filtered, dried (105 °C/24 h), and weighed to obtain the final dry mass. Solubility was expressed as a percentage, calculated from the difference between the initial and final dry mass.

*Mechanical Properties*

Mechanical tests were performed according to the ASTM method (D-882-91, 1996) [23], using an Autograph AGS 10 KN equipment, SHIMADZU (Kyoto, Japan). Films were cut into dimensions of 50 × 20 mm, and thickness was measured with a digital micrometer (Mitutoyo, Japan, 0.001 mm precision). The specimens were tensile-tested at a speed of 50 $mm.min^{-1}$, with an initial grip separation of 30 mm. The properties determined were maximum tensile strength (MPa), elongation at break (%), and modulus of elastic modulus (MPa) [4].

### Statistical analysis

Results were analyzed using STATISTICA StatSoft 8.0.360 software (Tulsa, USA). One-way analysis of variance (ANOVA) was used to study sample variation. Tukey's tests were conducted to determine differences between means with a 95% confidence level ($p < 0.05$).

## RESULTS

### Composition and Amylose Content of Pearl Millet Starch

The starch extracted by the alkaline method exhibited low residual levels of protein, lipids, and ash, indicating effective purification (Table 1).

**Table 1**. Proximate composition and amylose content of pearl millet starch.

| Component | Content (%) |
|---|---|
| Moisture | 10.76 ± 0.33 |
| Proteins | 1.03 ± 0.07 |
| Lipids | 0.11 ± 0.02 |
| Ash | 0.51 ± 0.01 |
| Carbohydrates | 87.59 |
| Amylose | 28.28 ± 0.83 |

Values are presented as mean ± standard deviation. Carbohydrate content was obtained by difference of 100%.

The material showed high carbohydrate content, confirming its high purity. The amylose content was within the range typically reported for millet starches, suggesting suitability for film formation due to its ability to promote cohesive and structured polymeric networks.

### Zeta Potential of the Suspension of Cellulose Nanofibrils

The colloidal stability of cellulose nanofibril (CNF) suspensions obtained from millet stalks was evaluated through zeta potential measurements at different dilutions. The values obtained are presented in Table 2.

**Table 2**. Zeta potential of the suspension of cellulose nanofibrils

| Dilutions of suspension | Zeta potential (mV) |
|---|---|
| 1:100 | -22.1 |
| 1:200 | -28.9 |
| 1:500 | -21.5 |
| 1:1000 | -31.2 |
| 1:2000 | -29.1 |

All samples presented absolute values above 20 mV, a threshold commonly associated with stable dispersions. Among the tested conditions, the dilutions of 1:200, 1:1000, and 1:2000 exhibited the highest absolute values, suggesting enhanced electrostatic stability compared to the more concentrated suspensions.

## Characterization of Biodegradable Films

*Thermogravimetric Analysis (TGA)*

The data relating to the thermal analysis of the films are presented through the thermogravimetric curves in Figure 1 and the data shown in Table 3.

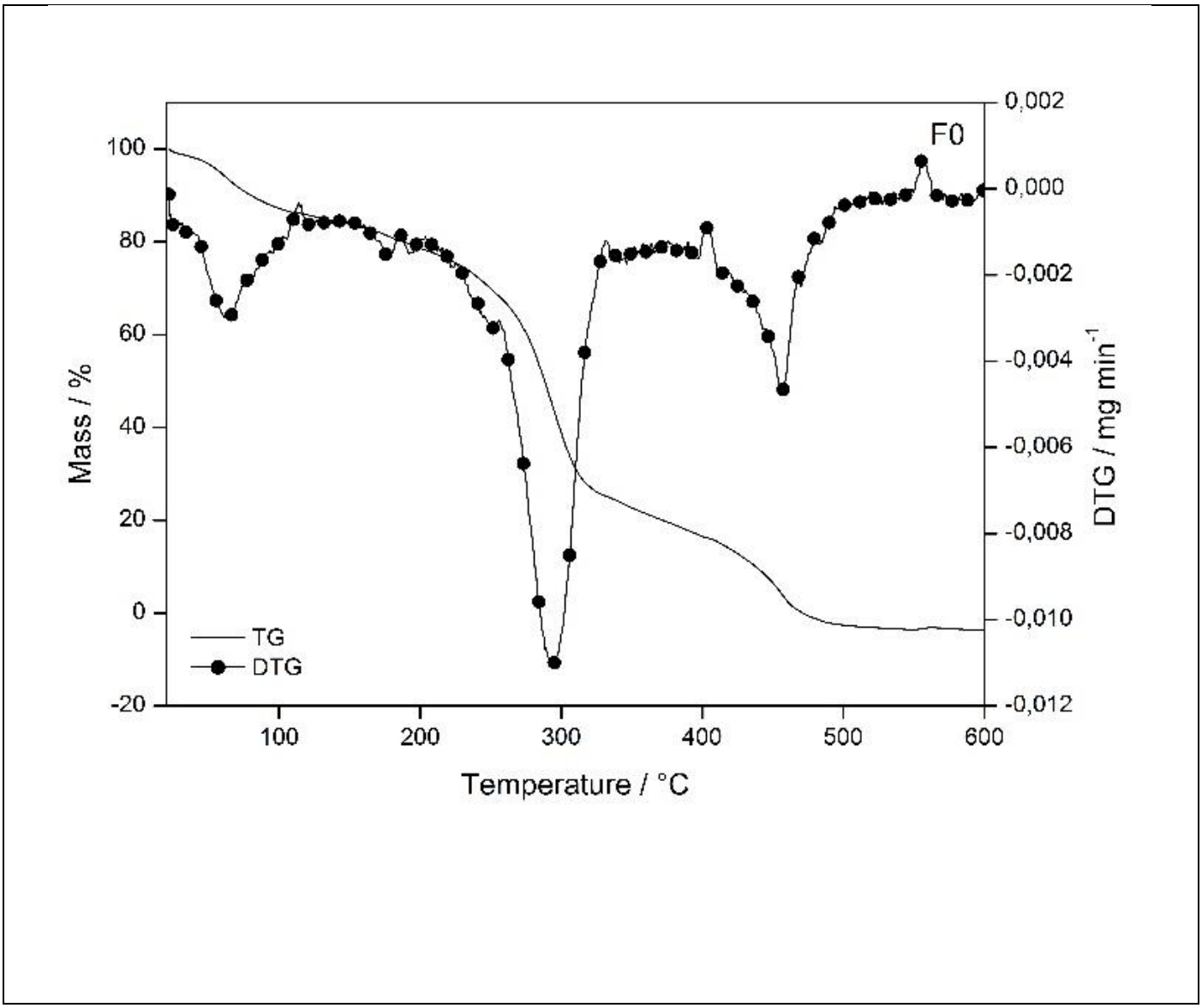

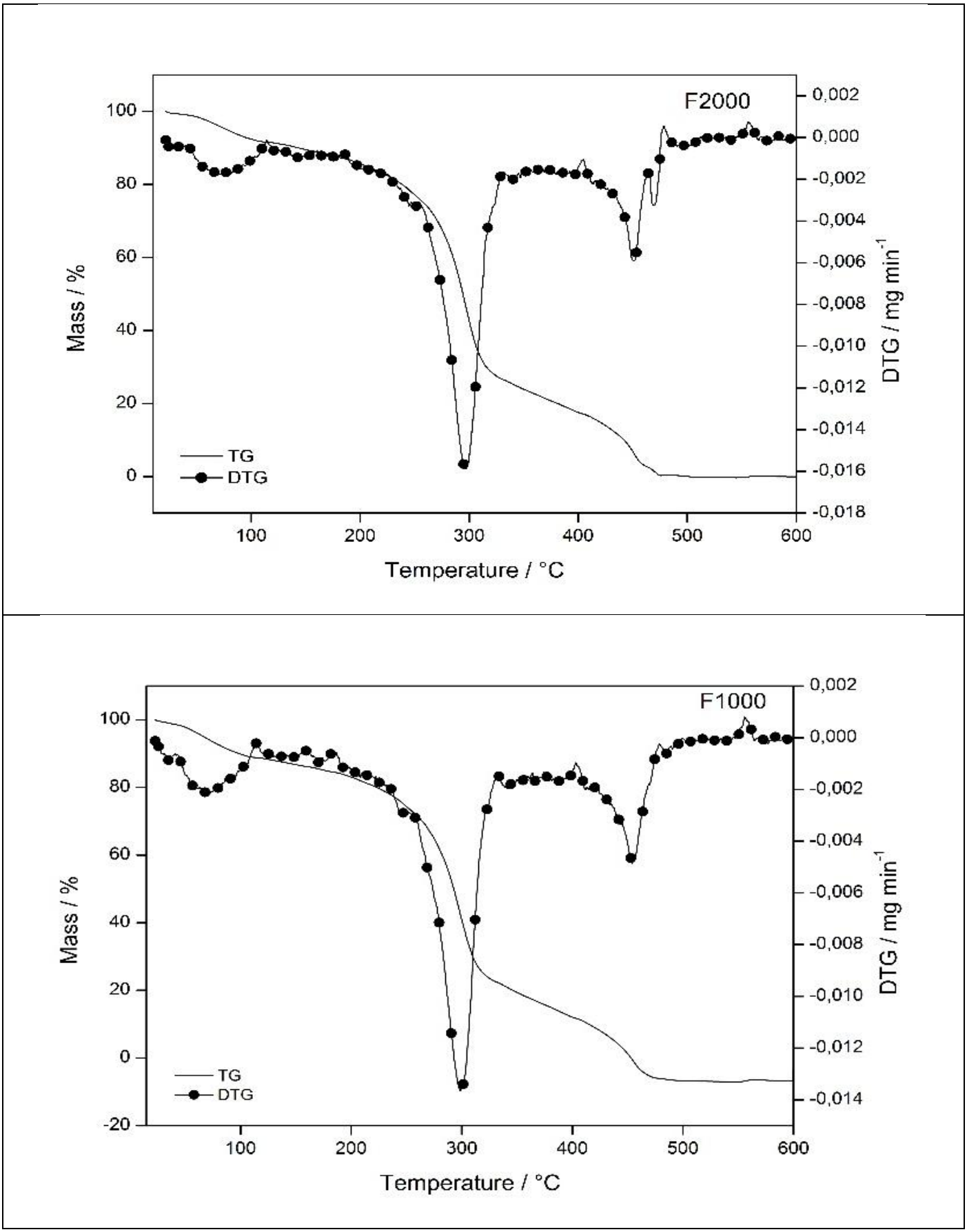
F2000
Mass / %
DTG / mg min-1
Temperature / °C
TG
DTG
100
80
60
40
20
0
0,002
0,000
-0,002
-0,004
-0,006
-0,008
-0,010
-0,012
-0,014
-0,016
-0,018
100
200
300
400
500
600
F1000
Mass / %
DTG / mg min-1
Temperature / °C
TG
DTG
100
80
60
40
20
0
-20
0,002
0,000
-0,002
-0,004
-0,006
-0,008
-0,010
-0,012
-0,014
100
200
300
400
500
600

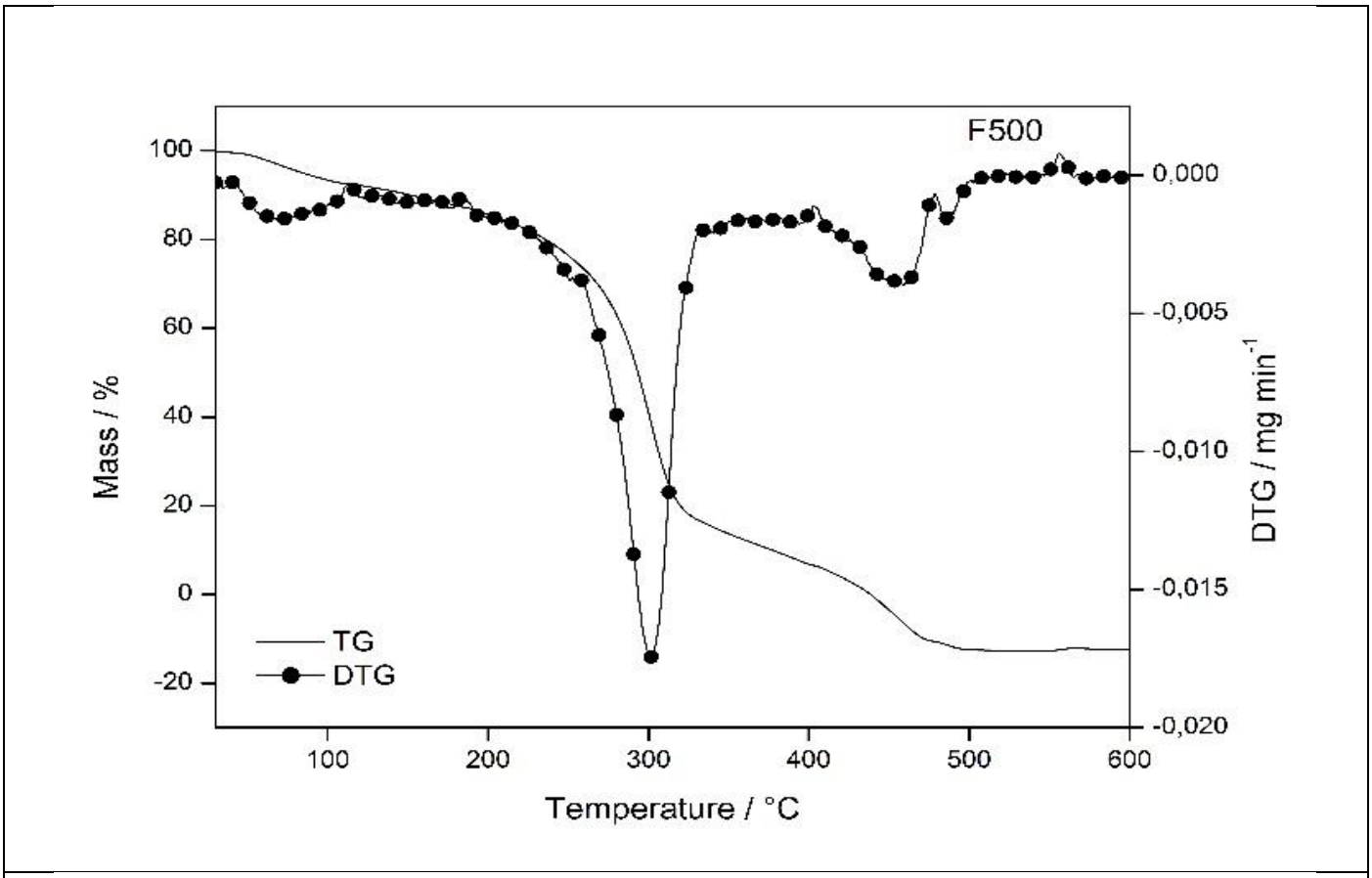
F500
Mass / %
DTG / mg min-1
Temperature / °C
TG
DTG
100
80
60
40
20
0
-20
100
200
300
400
500
600
0,000
-0,005
-0,010
-0,015
-0,020

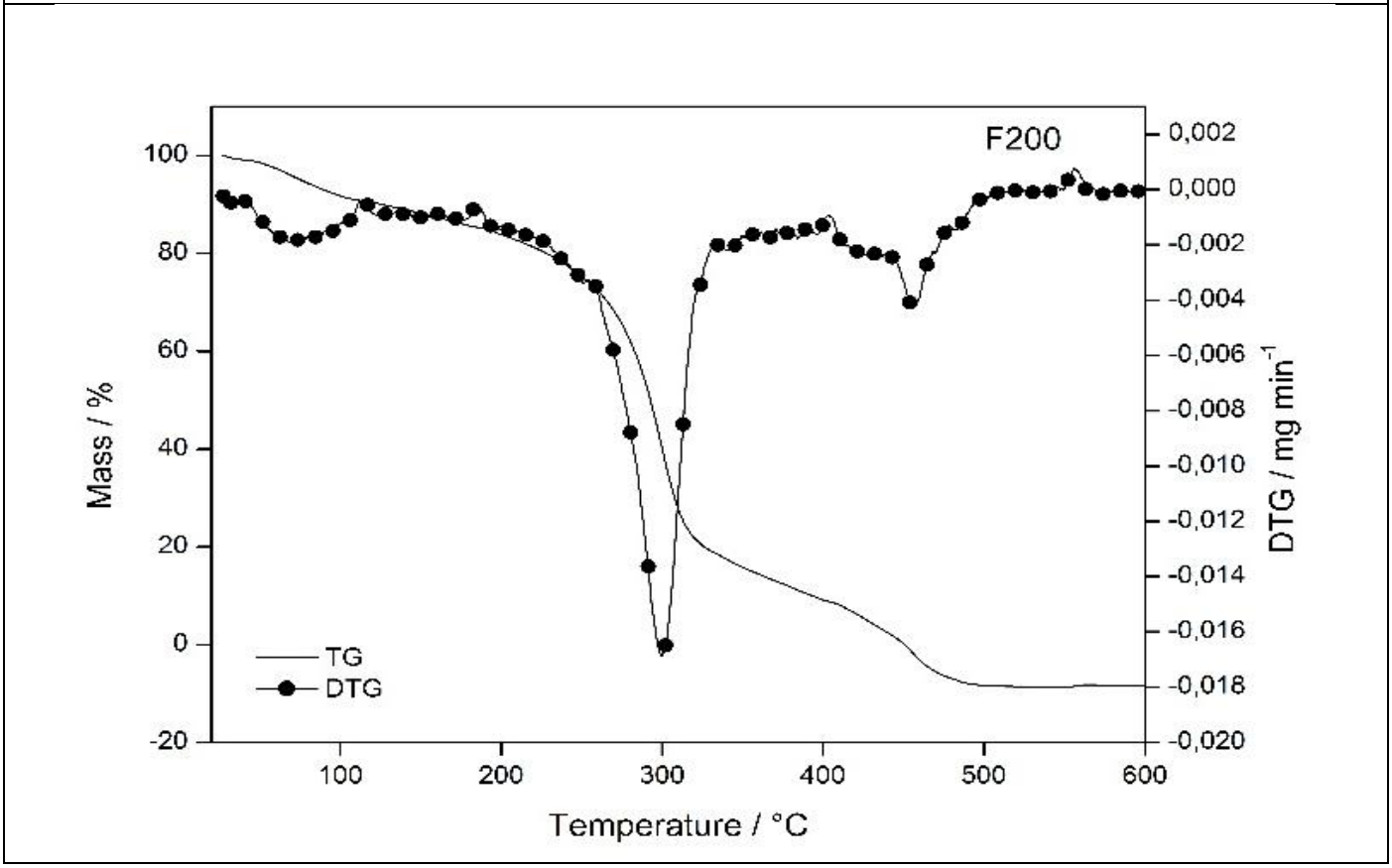
F200
Mass / %
DTG / mg min-1
Temperature / °C
TG
DTG
100
80
60
40
20
0
-20
100
200
300
400
500
600
0,002
0,000
-0,002
-0,004
-0,006
-0,008
-0,010
-0,012
-0,014
-0,016
-0,018
-0,020

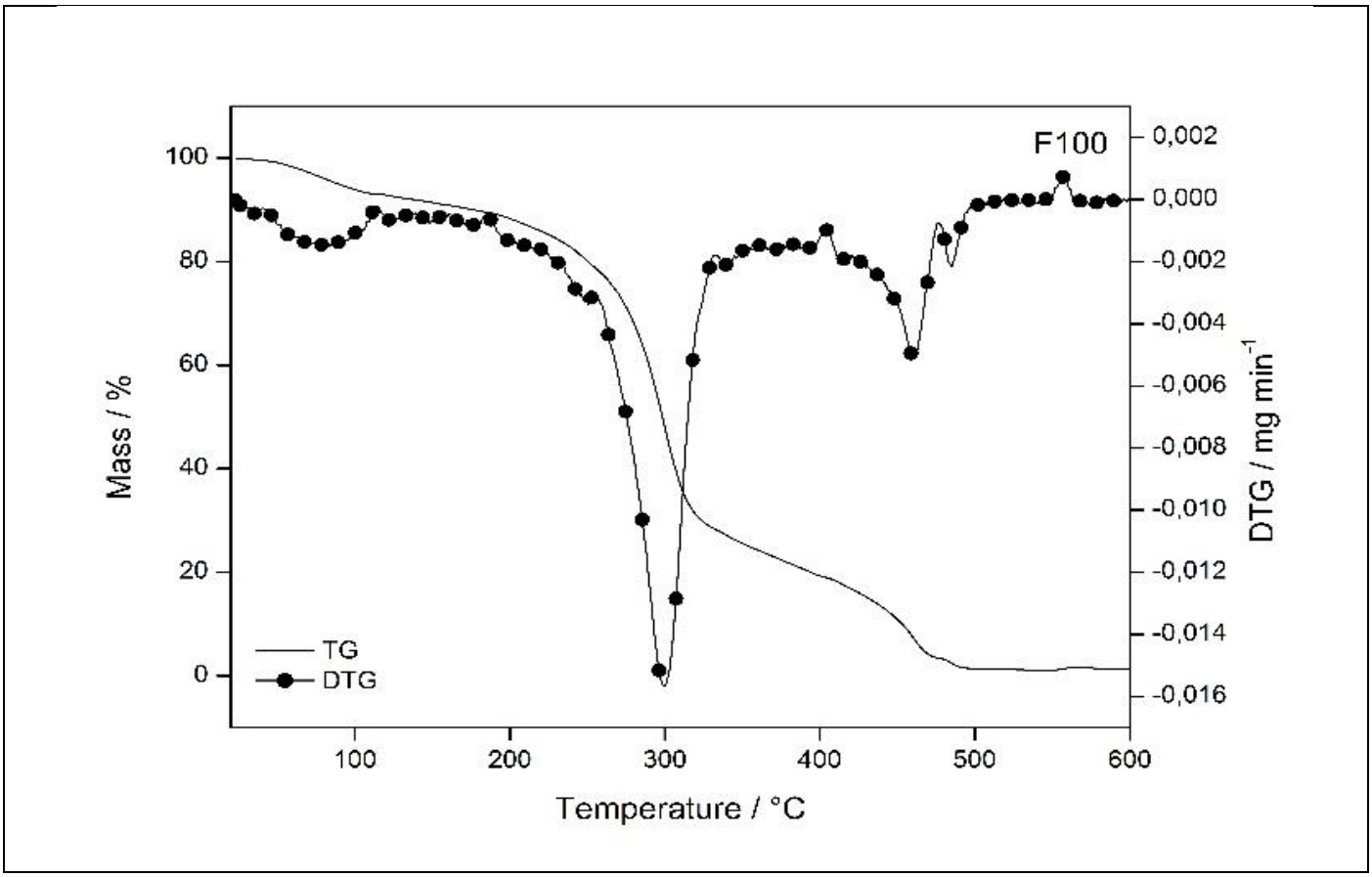


**Figure 1**. Thermogravimetric curves of the films F0, F2000, F1000, F500, F200, and F100.

**Table 3**. Results from TG/DTG of films

| Sample | Thermal event | 1º | 2º | 3º | 4º |
|---|---|---|---|---|---|
| F0 | Ti-Tf, °C | 30 – 113.46 | 160.49 – 206.94 | 225.99 – 330.15 | 406.90 – 492.01 |
| | Tp, °C | 63.48 | 178.35 | 293.20 | 456.31 |
| | Δm, % | 12.32 | 5.17 | 60.48 | 21.41 |
| F2000 | Ti-Tf, °C | 30 – 115.89 | 151.39 – 199.60 | 249.83 – 331.23 | 418.99 – 487.98 |
| | Tp, °C | 71.29 | 160.52 | 296.35 | 450.97 |
| | Δm, % | 9.66 | 4.78 | 63.41 | 21.42 |
| F1000 | Ti-Tf, °C | 30 – 115.29 | 157.06 – 197.38 | 236.56 – 333.63 | 403.06 – 480.25 |
| | Tp, °C | 71.36 | 160.86 | 298.51 | 454.05 |
| | Δm, % | 10.84 | 4.77 | 62.25 | 22.10 |
| F500 | Ti-Tf, °C | 30 – 115.00 | 162.34 – 212.27 | 251.29 – 330.48 | 411.68 – 477.96 |
| | Tp, °C | 71.15 | 183.02 | 301.29 | 458.35 |
| | Δm, % | 8.16 | 5.11 | 66.91 | 19.27 |
| F200 | Ti-Tf, °C | 30 – 112.82 | 164.57 – 201.73 | 246.61 – 332.09 | 407.56 – 495.61 |
| | Tp, °C | 68.68 | 185.18 | 299.80 | 455.73 |
| | Δm, % | 9.67 | 4.97 | 64.64 | 19.93 |
| F100 | Ti-Tf, °C | 30 – 115.56 | 149.54 – 189.86 | 257.82 – 333.40 | 421.09 – 501.15 |
| | Tp, °C | 81.74 | 160.96 | 299.73 | 459.78 |
| | Δm, % | 10.80 | 4.83 | 62.91 | 20.78 |

Δm = mass loss (%); Ti – Tf = initial and final temperature (°C); Tp = peak temperature.

Four main mass loss events were observed for all formulations. The first thermal event, associated with moisture loss, occurred at higher temperatures in CNF-containing films compared to the control, suggesting stronger water–matrix interactions promoted by nanofibril incorporation.

The second degradation stage showed minimal variation among formulations, indicating that CNF addition did not significantly affect the thermal behavior of the plasticizer. In contrast, the third event, corresponding to the main polymeric matrix degradation, was strongly influenced by CNF content. The F500 formulation exhibited the highest thermal stability, as evidenced by its elevated peak temperature, indicating more effective intermolecular interactions within the matrix.

In the final degradation stage, variations among samples reflected differences in residual carbon oxidation. Overall, the results demonstrate that CNF incorporation modifies the thermal degradation behavior of starch films, with intermediate concentrations providing the most favorable thermal performance.

*Scanning Electron Microscopy (SEM)*

Figure 2 presents the micrographs obtained for the different formulations.

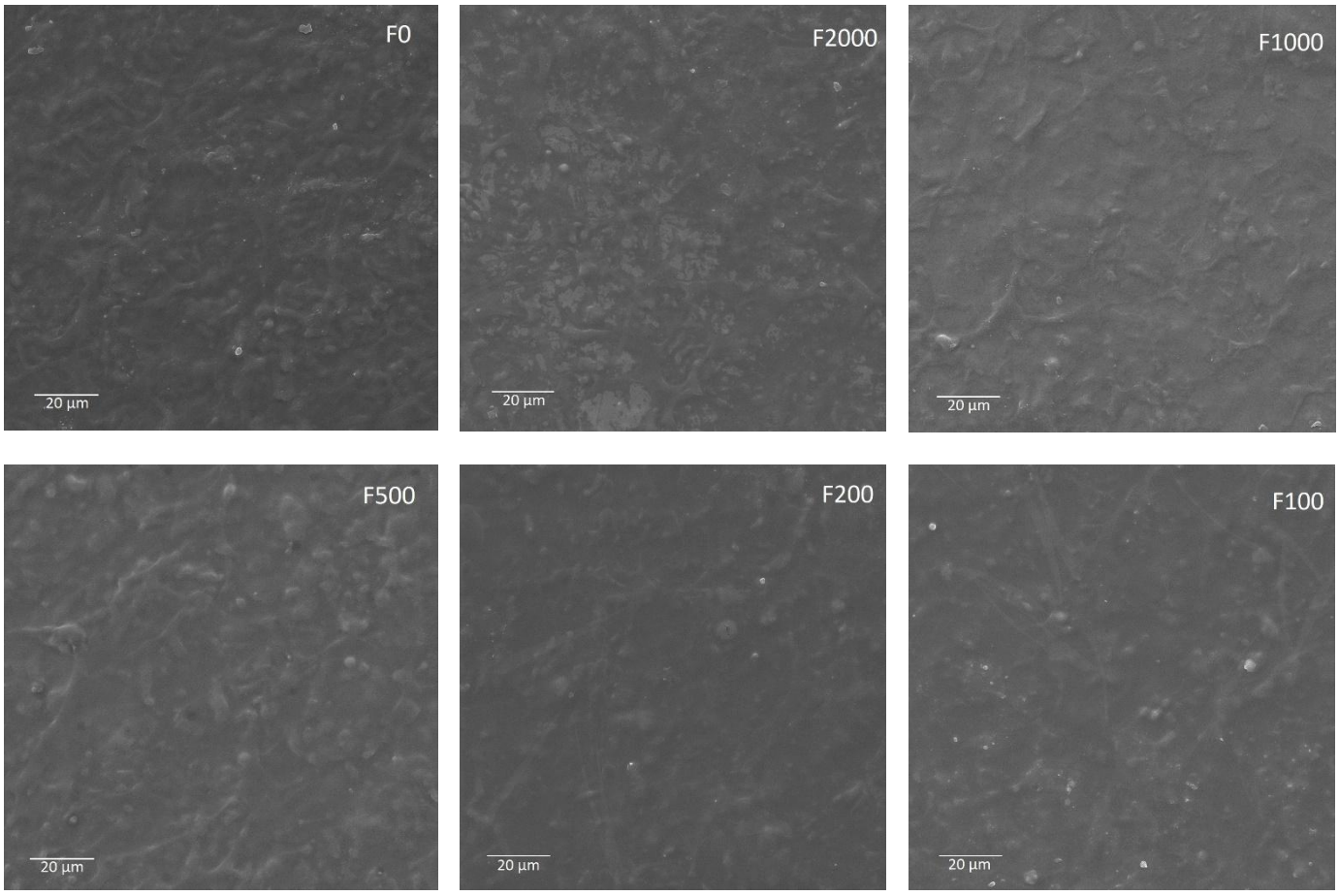


**Figure 2**. Microscopic images at 2000× magnification of films F0, F2000, F1000, F500, F200, and F100.

No significant differences were observed in water vapor permeability among the film formulations (Table 4). However, a decreasing trend was noted in CNF-containing samples compared to the control, although this effect was not statistically significant and should be interpreted with caution, suggesting that nanofibrils may contribute to reducing water vapor transmission.

Similarly, water solubility did not differ significantly among samples. Slight variations were observed depending on CNF concentration, with lower concentrations tending to result in reduced solubility. These findings indicate that CNF incorporation does not adversely affect the water resistance of the films, maintaining their structural stability in aqueous environments.

**Table 4**. Water vapor permeability and water solubility of films.

| Sample | Water vapor permeability (g. $Pa^{-1}.s^{-1}.m^{-1}$) | Water solubility (%) |
|---|---|---|
| F0 | $1.11\times10^{-10} \pm 1.80\times10^{-11}$ | 19.19 ± 0.46 |
| F2000 | $8.87\times10^{-11} \pm 7.16\times10^{-12}$ | 17.44 ± 1.97 |
| F1000 | $9.46\times10^{-11} \pm 1.85\times10^{-11}$ | 17.74 ± 0.02 |
| F500 | $9.61\times10^{-11} \pm 1.30\times10^{-12}$ | 18.91 ± 0.57 |
| F200 | $9.96\times10^{-11} \pm 8.71\times10^{-12}$ | 18.69 ± 0.19 |
| F100 | $9.56\times10^{-11} \pm 7.50\times10^{-12}$ | 19.47 ± 0.42 |

Data are expressed as mean ± standard deviation. No significant difference was observed (Tukey, $p > 0.05$).

*Mechanical Properties*

The mechanical properties of films were evaluated for tensile strength, elongation at break, and elastic modulus. Table 5 presents the values obtained for the different formulations.

**Table 5**. Mechanical properties data of the films

| Sample | Maximum tensile strength (Mpa) | Elongation at break (%) | Modulus of elasticity (Mpa) |
|---|---|---|---|
| F0 | 1.26 ± 0.12 $^{b}$ | 141.00 ± 24.72 $^{ab}$ | 47.06 ± 12.50 $^{bc}$ |
| F2000 | 1.36 ± 0.44 $^{b}$ | 96.60 ± 36.99 $^{b}$ | 65.85 ± 21.35 $^{abc}$ |
| F1000 | 1.30 ± 0.13 $^{b}$ | 160.64 ± 25.61 $^{a}$ | 93.99 ± 20.96 $^{a}$ |
| F500 | 2.47 ± 0.63 $^{a}$ | 118.12 ± 26.93 $^{ab}$ | 84.10 ± 11.89 $^{a}$ |
| F200 | 1.12 ± 0.11 $^{b}$ | 148.39 ± 16.42 $^{a}$ | 74.39 ± 31.13 $^{ab}$ |
| F100 | 0.97 ± 0.11 $^{b}$ | 131.64 ± 21.47 $^{ab}$ | 40.17 ± 10.46 $^{c}$ |

Data are expressed as mean ± standard deviation. Different letters in the same column indicate a significant difference between the samples (Tukey's test, $p \leq 0.05$).

The F500 formulation exhibited the best overall performance, with a marked increase in tensile strength, indicating an optimal reinforcement effect at intermediate nanofibril concentration. In contrast, films with higher CNF content showed reduced mechanical performance, likely due to the formation of agglomerates that act as structural defects.

Elongation at break remained relatively high across all formulations, indicating that film flexibility was preserved despite the addition of reinforcing material. An increase in elastic modulus was observed in selected formulations, reflecting enhanced stiffness of the polymeric matrix. These results demonstrate that CNF incorporation improves mechanical performance when properly dispersed, with intermediate concentrations providing the most balanced combination of strength and flexibility.

## DISCUSSION

### Composition and Amylose Content of Pearl Millet Starch

The alkaline extraction method proved efficient, yielding low residual protein and lipid contents in the extracted starch. Millet seeds of the species *Cenchrus americanus* (L.) Morrone typically contain 9-15% protein [24-26], and the residual value obtained confirms NaOH effectiveness in solubilizing proteins strongly associated with starch granules [27-28]. Similar results were reported with 1.26% residual protein when extracting proso millet starch by alkaline method [29].

Regarding lipids, millet seeds present contents ranging from 2.7 to 7% [24-26]. The residual content of 0.11% evidences highly efficient removal, superior to the 0.84% reported [29]. This efficacy is particularly relevant since lipids can compromise starch functional properties through formation of inclusion complexes with amylose, limiting granule expansion during gelatinization and reducing swelling power and peak viscosity [7,30]. The efficient removal is attributed to lipid saponification by NaOH, converting them into water-soluble compounds easily eliminated during washing [31].

The moisture content of 10.76% is aligned with the value reported for others millet starch [32]. The low ash content (0.51%) may correspond to inorganic carbonates, silicates, and phosphates, in addition to minerals such as phosphorus, potassium, and magnesium typically present in millet [26,33]. The carbohydrate content of 87.59% reflects the high purity of the extracted starch [24,25].

The amylose content of 28.28% is within the 28-38% range reported for millet starches in the literature [1,5] and close to the 31.32% found for native pearl millet starch [34]. This value can be considered high when compared to other starchy sources such as corn, wheat, and potato [35], conferring advantages for applications in biodegradable films. The linear structure of amylose favors the formation of uniform and compact polymeric matrices, resulting in greater mechanical strength, thermal stability, and water vapor barrier properties [1,5].

Variations in amylose content among different studies, such as the 20-28% reported for different pearl millet genotypes [36], can be attributed to differences in botanical source, cultivation conditions, and starch extraction methods [37]. The amylose content directly influences the structural organization of granules, affecting amylopectin packing into crystals, crystalline lamellae organization, and consequently properties such as water absorption capacity, gelatinization temperature, and thermal behavior [35,38].

## Zeta Potential of the Suspension of Cellulose Nanofibrils

Zeta potential is a fundamental measure for evaluating colloidal suspension stability, representing the electrical potential difference between the liquid medium and the particle shear plane [39]. High absolute values indicate that Coulomb repulsive forces overcome attractive van der Waals forces, suggesting a tendency toward colloidal stability under the evaluated conditions**.** The literature establishes that absolute values above ±20 mV are favorable for colloidal stability [4,40].

All dilutions analyzed in this study presented zeta potential with absolute values above 20 mV, ranging from -21.5 to -31.2 mV, indicating potential colloidal stability under the measurement conditions. The negative charge is characteristic of cellulose nanofibrils, due to hydroxyl and carboxyl groups ($-COO^-$) introduced during oxidative processing. Similar values (-21 to -25.9 mV) were obtained for nanocrystalline cellulose from cassava bagasse [40].

Dilutions of 1:200, 1:1000 and 1:2000 exhibited the highest absolute values, indicating superior stability, comparable to the -23.53 mV reported for millet bran CNF [39]. High aspect ratios, characterized by small diameters and great fiber length, generally intensify van der Waals forces, resulting in greater tendency to particle aggregation

More concentrated dilutions (not shown in Table 2) presented zeta potential outside stability criteria, indicating low stability and aggregation, which made homogeneous film formation unfeasible. Overall, millet CNF suspensions at the evaluated dilutions present adequate zeta potential values, which suggest favorable dispersion at the colloidal level; however, these results alone are not sufficient to ensure stability during film processing, where factors such as concentration, shear, and drying conditions may influence nanofibril aggregation**.** This limitation is consistent with the SEM observations, where agglomerates were detected at higher CNF concentrations, reinforcing that zeta potential alone does not fully predict dispersion behavior in the obtained films.

## Characterization of Biodegradable Films

### *Thermogravimetric Analysis (TGA)*

Thermogravimetric analysis revealed that CNF incorporation alters the thermal degradation profile of millet starch films. Four main mass loss events were observed for all formulations.

The first event (<115 °C), associated with moisture loss, showed lower peak temperature for the control film F0 compared to CNF films, indicating weaker water binding in the control matrix. CNF introduction, a material rich in hydroxyl groups, increases the density of these groups in the matrix, promoting stronger hydrogen bonds with water and raising peak temperatures [41-43]. The lower mass loss in CNF films, particularly in F500, suggests an alteration in the free-to-bound water ratio, indicating optimized starch-cellulose interactions [44].

The second event (150-210 °C), attributed to glycerol degradation, showed minimal variation among samples, as plasticizer concentration was kept constant. This behavior confirms that CNF addition does not significantly interfere with plasticizer decomposition [4,43]. The third event (225-335 °C) corresponds to the main polymeric matrix decomposition. Sample F500 stood out with the highest peak temperature and mass loss, indicating superior thermal stability and more complete degradation. This behavior is attributed to the

formation of an efficient network of hydrogen bond interactions between starch and CNF, which requires greater energy to be disrupted [42,45].

The fourth event (>400 °C) involves combustion of carbonaceous residual material. Samples F0, F1000, and F2000 showed higher residue oxidation, while F500 left minimal residue, confirming its more complete decomposition in the third event [4,42]. The results demonstrate that CNF incorporation, particularly at the intermediate concentration F500, increases the thermal stability of films and promotes stronger polymer interactions, confirming its potential for applications requiring greater thermal resistance.

*Scanning Electron Microscopy (SEM)*

Morphological analysis revealed that the control film (F0) presented a continuous, uniform surface free from cracks, compatible with starch matrices described in the literature [43,45]. Nanocomposite films exhibited a continuous surface without cracks, but with slight roughness, a common characteristic in CNF-containing films [41,43]. The absence of irregularities such as cracks indicates adequate gelatinization and processing.

In films with higher CNF concentrations (F200 and F100), elongated bundles corresponding to incompletely dispersed nanofibril agglomerates were observed. This phenomenon relates to electrostatic stability, since F100 presented the lowest zeta potential (Table 2), indicating lower dispersion tendency. Similar results were reported for nanocomposites with high reinforcement concentrations [45,46].

Despite the agglomerates, good adhesion between nanofibrils and matrix was observed, with fibers coated by starch, indicating favorable interaction. This behavior is attributed to the chemical similarity between starch and cellulose, both hydroxyl-rich polysaccharides that form strong hydrogen bonds [22,43]. The presence of agglomerates at higher concentrations indicates the need for dispersion method optimization, as such irregularities may affect the mechanical and barrier properties of the films.

*Water Vapor Permeability and Water Solubility*

The water vapor permeability values obtained are comparable to those reported in the literature for starch films and their nanocomposites, indicating that the films present properties within the expected range for such materials [3, 47]. Although no statistically significant differences were observed**,** the trend of WVP reduction in nanocomposite films, especially F2000 (~20% reduction), may be associated to the "tortuous path theory", well-dispersed nanofibrils act as physical barriers that fill voids in the matrix, creating longer pathways for water molecule diffusion [43,45]. Additionally, strong hydrogen bond interactions between CNF and starch reduce free spaces at the interface where water could diffuse [22].

Regarding solubility, the values obtained are compatible with the literature for starch films with CNF (16-30%) [8,43]. Comparatively, pure starch films described in the literature present higher solubility (30-38%) [47], revealing that the control film F0 (19.19%) already presents notably low solubility. This characteristic is relevant in the context of food packaging applications, where structural integrity must be maintained even under high humidity.

The apparent superior performance of F2000 (lowest WVP and lowest solubility) should be interpreted cautiously, given the absence of statistical significance**,** and suggests that at the most diluted concentration, nanofibrils dispersed efficiently in the matrix, aligning with observations on optimized nanofiller concentrations [3,45]. The trend of lower solubilities at lower CNF concentrations (F2000, F1000) and higher solubility at the highest concentration (F100) can be explained by the hydrophilic nature of cellulose. At higher concentrations, additional hydroxyl groups increase the material's affinity for water, potentially overlapping with the physical barrier effect of the network [42].

*Mechanical Properties*

Mechanical properties are critical parameters for the application of biodegradable films in packaging, determining their ability to withstand stresses during handling, transport, and storage [3].

Tensile strength varied significantly, with F500 standing out with the highest value (2.47 MPa), indicating that the intermediate CNF concentration promoted the best reinforcement effect in the starch matrix. This increase is related to strong hydrogen bond interactions between starch and cellulose, which allow efficient stress transfer from the matrix to the nanofibrils [42,45]. In contrast, F100 presented the lowest strength, suggesting that excess CNF leads to agglomerate formation that acts as stress concentration points, weakening the structure [45,46], consistent with micrographs revealing agglomerates at higher concentrations.

Elongation at break, reflecting film flexibility, was high in all formulations (96-160%) compared to literature (50-70%) [4,8]. F1000 and F200 presented the highest values, with F1000 combining high elongation and strength equivalent to the control, suggesting that well-dispersed nanofibrils may contain cracks and absorb energy without compromising flexibility [22]. The lower elongation of F2000 indicates that very low concentrations may not form an efficient percolated network, generating localized weak points [45].

Elastic modulus, indicative of stiffness, was higher in F1000 and F500, significantly superior to the control, confirming that CNF makes the matrix more rigid [3]. F100 presented the lowest modulus, reinforcing that excess cellulose, with agglomerate formation, compromises stiffness by creating discontinuities in the matrix [46].

The combined analysis reveals that F500 presents the best overall mechanical performance, with significant gains in strength without compromising flexibility. F1000 also stands out, combining high stiffness and elongation. In contrast, F2000 and F100 represent the less favorable extremes: the former with insufficient concentration for reinforcement, and the latter with excess leading to agglomeration and weakening. The results confirm that CNF addition promotes significant improvements in mechanical properties provided the concentration is properly optimized.

Although the results demonstrate promising physicochemical and mechanical properties, the present study provides an initial assessment of the material. Further studies addressing optical properties, biodegradation behavior, migration aspects, and performance under real storage conditions are necessary to fully support its application in food packaging.

## CONCLUSION

This study highlighted the utilization of pearl millet as a renewable and viable source, through the development of biodegradable films based on starch extracted from pearl millet seeds and reinforced with cellulose nanofibrils obtained from the stalk, thereby adding value to this high-potential cereal. The films produced exhibited promising characteristics, notably the direct influence of cellulose nanofibril concentration on the evaluated properties.

The intermediate concentration (F500) provided the best balance of thermal, and mechanical properties, while barrier properties did not show statistically significant differences among formulations**.** High concentrations (F100) resulted in a loss of mechanical performance, due to nanofibril agglomeration, while low concentrations (F2000) compromised film flexibility, without affecting the water vapor barrier**.**

Given the observed properties, the developed films, upon optimization, may show potential for applications in low- and intermediate-moisture food packaging. Thus, this research contributes to the advancement of the field of biodegradable materials.

**Author Contributions:** Conceptualization, I.M.D. and L.G.L.; methodology, L.C.R., J.B.O., I.V. and L.A.P.; software, I.M.D., L.C., L.C.R. and S.S.R.; validation, L.G.L., L.C.R., L.C. and S.S.R.; formal analysis, L.C.; investigation, L.C.R. and L.C.; resources, L.G.L., J.B.O., I.V. and L.A.P.; data curation, L.C.R., L.C. and S.S.R.; writing—original draft preparation, L.C.R.; writing—review and editing, L.G.L. and J.B.O.; visualization, L.C.R.; supervision, L.G.L.; project administration, L.G.L.; funding acquisition, L.G.L. All authors have read and agreed to the published version of the manuscript.

**Funding:** This research received no external funding.

**Institutional Review Board Statement:** Not applicable.

**Informed Consent Statement:** Not applicable**.**

**Data Availability Statement:** Research data are only available upon request for corresponding author.

**Acknowledgments:** The authors thank the Coordenação de Aperfeiçoamento de Pessoal de Nível Superior (CAPES), the Multiuser Laboratories of the State University of Ponta Grossa for technical support and the Department of Forest Engineering and Technology, Federal University of Paraná.

**Conflicts of Interest:** The authors declare no conflict of interest.

**Use of Generative Artificial Intelligence**

The authors declare that large language models and other generative artificial intelligence (AI) or AI-assisted technologies cannot be credited as authors and have not been listed as authors of this paper.

The authors declare that no generative artificial intelligence (AI) or AI-assisted technologies were used to generate or modify the scientific content of this manuscript, including the conception of the study, data collection, data analysis, interpretation of results, or creation of original text, figures, tables or graphical abstracts, apart from routine tools for spelling, grammar checking and reference management that do not create original scholarly content.

## REFERENCES


1. Gautam N, Garg S, Yadav S. [Underutilized finger millet crop for starch extraction, characterization, and utilization in the development of flexible thin film]. J Food Sci Technol. 2021; 58:4411-9. https://doi.org/10.1007/s13197-020-04926-0
2. Ali A, Bairagi S, Ganie SA, Ahmed S. [Polysaccharides and proteins based bionanocomposites as smart packaging materials: from fabrication to food packaging applications: a review]. Int J Biol Macromol. 2023; 252:126534. https://doi.org/10.1016/j.ijbiomac.2023.126534
3. Bangar SP, Whiteside WS, Dunno KD, Cavender GA, Dawson P. [Pearl millet starch-based nanocomposite films reinforced with kudzu cellulose nanocrystals and essential oil: effect on functionality and biodegradability]. Food Res Int. 2022; 157:111384. https://doi.org/10.1016/j.foodres.2022.111384
4. Almeida VS, Barretto BRV, Maulucelli L, Carvalho Filho MAS, Demiate IM, Pinheiro LA, et al. [Thermal, morphological, and mechanical properties of regular and waxy maize starch films reinforced with cellulose nanofibers (CNF)]. Mater Res. 2020;23(2):e20190576. https://doi.org/10.1590/1980-5373-mr-2019-0576
5. Zhu F. [Structure, physicochemical properties, and uses of millet starch]. Food Res Int. 2014; 64:200-11. https://doi.org/10.1016/j.foodres.2014.06.026
6. Dias-Martins AM, Pessanha KLF, Pacheco S, Rodrigues JAS, Carvalho CWP. [Potential use of pearl millet (*Pennisetum glaucum* (L.) R. Br.) in Brazil: food security, processing, health benefits and nutritional products]. Food Res Int. 2018; 109:175-86. https://doi.org/10.1016/j.foodres.2018.04.023
7. Mahajan P, Bera MB, Panesar PS, Chauhan A. [Millet starch: a review]. Int J Biol Macromol. 2021; 180:61-79. https://doi.org/10.1016/j.ijbiomac.2021.03.063
8. Bangar SP, Siroha AK, Nehra M, Trif M, Ganwal V, Kumar S. [Structural and film-forming properties of millet starches: a comparative study]. Coatings. 2021;11(8):954. https://doi.org/10.3390/coatings11080954
9. Dominic CDM, Raj V, Neenu KV, Begum PMS, Formela K, Saeb MR, et al. [Chlorine-free extraction and structural characterization of cellulose nanofibers from waste husk of millet (*Pennisetum glaucum*)]. Int J Biol Macromol. 2022; 206:92-104. Doi: 10.1016/j.ijbiomac.2022.02.078
10. Wang H, Yang Q, Ferdinand U, Gong X, Qu Y, Gao W, et al. [Isolation and characterization of starch from light yellow, orange, and purple sweet potatoes]. Int J Biol Macromol. 2020; 160:660-8. https://doi.org/10.1016/j.ijbiomac.2020.05.259
11. Arns B, Bartz J, Radunz M, Evangelho JA, Pinto VZ, Zavareze ER, et al. [Impact of heat-moisture treatment on rice starch, applied directly in grain paddy rice or in isolated starch]. LWT Food Sci Technol. 2015;60(2):708-13. https://doi.org/10.1016/j.lwt.2014.10.059
12. Instituto Adolfo Lutz (IAL). [Physicochemical methods for food analysis]. 1st electronic ed. São Paulo: IAL; 2008. Available from: https://www.ial.sp.gov.br/resources/editorinplace/ial/2016_3_19/analisedealimentosial_2008.pdf
13. Demiate IM, Figueroa AM, Zortéa Guidolin MEB, Rodrigues dos Santos TP, Yangcheng H, Chang F, et al. [Physicochemical characterization of starches from dry beans cultivated in Brazil]. Food Hydrocoll. 2016; 61:812-20. https://doi.org/10.1016/j.foodhyd.2016.07.014
14. Dresch AP, Cavali M, Santos DF, Fogolari OO, Tironi SP, Pinto VZ, et al. [Different treatments of pearl millet for cellulose recovery: effects on lignocellulosic composition] [Preprint]. 2022 [cited 2024 Jun 28]. Available from: https://doi.org/10.21203/rs.3.rs-1689771/v1
15. Magalhães WLE, Claro FC, Matos M, Lengowski EC. [Production of cellulose nanofibrils by mechanical defibrillation in a colloidal mill]. Colombo: Embrapa; 2017. (Technical Communication 404).
16. Jhan F, Shah A, Gani A, Ahmad M, Noor N. [Nano-reduction of starch from underutilized millets: effect on structural, thermal, morphological and nutraceutical properties]. Int J Biol Macromol. 2020; 159:1113-21. https://doi.org/10.1016/j.ijbiomac.2020.05.020
17. Fan H, Ji N, Zhao M, Xiong L, Sun Q. [Characterization of starch films impregnated with starch nanoparticles prepared by 2,2,6,6-tetramethylpiperidine-1-oxyl (TEMPO)-mediated oxidation]. Food Chem. 2016; 192:865-72. https://doi.org/10.1016/j.foodchem.2015.07.093
18. Olivato JB, Marini J, Yamashita F, Pollet E, Grossmann MVE, Avérous L. [Sepiolite as a promising nanoclay for nano-biocomposites based on starch and biodegradable polyester]. Mater Sci Eng C. 2017; 70:296-302. https://doi.org/10.1016/j.msec.2016.08.077
19. Romko SS, Bet CD, Bach D, Bisinella RZB, Schnitzler E. [Thermal and structural evaluation of physically modified starch from loquat seeds (*Eriobotrya japonica Lindl.*)]. Asian J Sci Technol. 2025; 16(1):13362-71.
20. Bet CD, Oliveira CS, Colman TAD, Marinho MT, Lacerda LG, Ramos AP, et al. [Organic amaranth starch: a study of its technological properties after heat-moisture treatment]. Food Chem. 2018; 264:435-42. https://doi.org/10.1016/j.foodchem.2018.05.021

21. ASTM - American Society for Testing and Materials. [Standard test methods for water vapor transmission of material - E-96-95]. Philadelphia: ASTM; 1995.
22. Pelissari FM, Andrade-Mahecha MM, Sobral PJDA, Menegalli FC. [Nanocomposites based on banana starch reinforced with cellulose nanofibers isolated from banana peels]. J Colloid Interface Sci. 2017; 505:154-67. https://doi.org/10.1016/j.jcis.2017.05.106
23. ASTM - American Society for Testing and Materials. [Standard test methods for tensile properties of thin plastic sheeting - D-882-91]. Philadelphia: ASTM; 1996.
24. Food and Agriculture Organization (FAO). [Millets 2023: FAO is the lead agency for promoting millets to improve food security, nutrition, and resilience in the face of climate change] [Internet]. Rome: FAO; 2023 [cited 2024 Jun 28]. Available from: https://www.fao.org/millets-2023/en
25. Khalil I, Bashir S, Saeed K, Alsulami T, Rafique H, Mukonzo EKL. [Phytochemical and structural portrayal of barley and pearl millet through FTIR and SEM]. Food Sci Nutr. 2025;13(5): e70120. https://doi.org/10.1002/fsn3.70120
26. Pavas, Suman, Majumdar AD, Munjal N, Kamboj U. [Characterization of *Pennisetum glaucum* (pearl millet)]. J Phys Conf Ser. 2022; 2267:012020. https://doi.org/10.1088/1742-6596/2267/1/012020
27. Kumar SR, Tangsrianugul N, Suphantharika M. [A review on isolation, characterization, modification, and applications of proso millet starch]. Foods. 2023;12(12):2413. https://doi.org/10.3390/foods12122413
28. Majumder S, Saha J, Karmakar S, Gupta A, Banerjee S, Banerjee S, et al. [Characterization of starch from minor millets and its potential applications: a review]. Int J Biol Macromol. 2024; 254:127890.
29. Sandhiya R, Buvaneswaran M, Sunil CK. [Effect of annealing and ultrasound treatments on physicochemical, functional, thermal, and structural properties of proso millet starch]. Discov Food. 2025; 5:49. https://doi.org/10.1007/s44187-025-00323-8
30. Ai Y, Jane J. [Understanding starch structure and functionality]. In: Sjöö M, Nilsson L, editors. Starch in food: structure, function and applications. 2nd ed. Cambridge: Woodhead Publishing; 2018. p. 151-78. https://doi.org/10.1016/b978-0-08-100868-3.00003-2
31. Pires MB, Amante ER, Petkowicz CLO, Esmerino EA, Rodrigues AMC, Silva LHM. [Impact of extraction methods and genotypes on the properties of starch from peach palm (*Bactris gasipaes* Kunth) fruits]. LWT Food Sci Technol. 2021; 150:111983. https://doi.org/10.1016/j.lwt.2021.111983
32. Gupta R, Gaur S. [Investigating the effect of natural fermentation in modifying the physico-functional, structural and thermal characteristics of pearl and finger millet starch]. J Sci Food Agric. 2024;104(4):2440-8. https://doi.org/10.1002/jsfa.13129
33. Bhatt P, Kumar V, Rastogi H, Malik MK, Dixit R, Garg S, et al. [Functional and tableting properties of alkali-isolated and phosphorylated barnyard millet (*Echinochloa esculenta*) starch]. ACS Omega. 2023;8(3):30294-305. https://doi.org/10.1021/acsomega.3c03158
34. Kaur P, Annapure US. [Effects of pin-to-plate atmospheric cold plasma for modification of pearl millet (Pennisetum glaucum) starch]. Food Res Int. 2023; 169:112930. https://doi.org/10.1016/j.foodres.2023.112930
35. Cornejo-Ramírez YI, Martínez-Cruz O, Del Toro-Sánchez CL, Wong-Corral FJ, Borboa-Flores J, Cinco-Moroyoqui FJ. [The structural characteristics of starches and their functional properties]. CyTA J Food. 2018;16(1):1003-17. https://doi.org/10.1080/19476337.2018.1518343
36. Krishnan V, Awana M, Singh A, Goswami S, Vinutha T, Kumar RR, et al. [Starch molecular configuration and starch-sugar homeostasis: key determinants of sweet sensory perception and starch hydrolysis in pearl millet (*Pennisetum glaucum*)]. Int J Biol Macromol. 2021; 183:1087-95. https://doi.org/10.1016/j.ijbiomac.2021.05.004
37. Sultana A, Bangar SP, Whiteside WS. [Effect of stearic acid modification on properties of pearl millet starch]. Biomass Convers Biorefin. 2025; 15:8745-53. https://doi.org/10.1007/s13399-024-05623-0
38. Yashini M, Khushbu S, Madhurima N, Sunil CK, Mahendran R, Venkatachalapathy N. [Thermal properties of different types of starch: a review]. Crit Rev Food Sci Nutr. 2022;64(2):1-24. https://doi.org/10.1080/10408398.2022.2141680
39. Zhu Y, Wei Z, Jiang F, Hu W, Yu X, Du S. [Comparative analysis of millet bran nanocelluloses with various morphologies: revealing differences in the formation mechanism and structure characteristics]. Carbohydr Polym. 2024; 342:122419. https://doi.org/10.1016/j.carbpol.2024.122419
40. Travalini AP, Prestes E, Pinheiro LA, Demiate IM. [Extraction and characterization of nanocrystalline cellulose from cassava bagasse]. J Polym Environ. 2018; 26:789-97. https://doi.org/10.1007/s10924-017-0983-8
41. Marques GS, Carvalho GR, Marinho NP, Muniz GIB, Jorge LMM, Jorge RMM. [Production and characterization of starch-based films reinforced by ramie nanofibers (*Boehmeria nivea*)]. J Appl Polym Sci. 2019;136(4):47919. https://doi.org/10.1002/app.47919
42. Travalini AP, Lamsal B, Magalhães WLE, Demiate IM. [Cassava starch films reinforced with lignocellulose nanofibers from cassava bagasse]. Int J Biol Macromol. 2019; 139:1151-61. https://doi.org/10.1016/j.ijbiomac.2019.08.115
43. Daza-Orsini SM, Medina-Jaramillo C, Caicedo-Chacon WD, Ayala-Valencia G, López-Córdoba A. [Isolation of taro peel cellulose nanofibers and its application in improving functional properties of taro starch nanocomposites films]. Int J Biol Macromol. 2024;273(Pt 2):132951. https://doi.org/10.1016/j.ijbiomac.2024.132951

44. Chavan P, Singh GP, Aayush K, Sharma S, Chauhan PK, Thory R, et al. [Development and characterization of pearl millet (AHB 1200) starch nanoparticle-based edible films: a paradigm shifts in food packaging]. J Food Process Eng. 2024;47(2): e14575. https://doi.org/10.1111/jfpe.14575
45. Bhardwaj M, Bist Y, Saxena DC. [Effect of amylose content and starch nanocrystals on the structure-function properties of pearl millet starch nanocomposite films]. Food Biophys. 2025; 20:169. https://doi.org/10.1007/s11483-025-10058-9
46. Tian J, Kong Y, Qian S, Zhang Z, Xia Y, Li Z. [Mechanically robust multifunctional starch films reinforced by surface-tailored nanofibrillated cellulose]. Compos B Eng. 2024; 275:111339. https://doi.org/10.1016/j.compositesb.2024.111339
47. Choudhary A, Kumar M, Chaudhary V. [Isolation and characterization of starch from underutilized barnyard millet (*Echinochloa frumentacea*) and its utilization in the development of biopolymer film]. J Food Meas Charact. 2025;19:8770-84. https://doi.org/10.1007/s11694-025-03455-8